

# A Nonlinear Potential-Flow Model For Wave-Structure Interaction Using High-Order Finite Differences On Overlapping Grids

Mostafa Amini-Afshar<sup>\*1</sup>, Harry B. Bingham<sup>1</sup>, William D. Henshaw<sup>2</sup>, and Robert Read<sup>1</sup>

<sup>1</sup>Department of Mechanical Engineering, Technical University of Denmark

Section for Fluid Mechanics, Coastal and Maritime Engineering

\*maaf@mek.dtu.dk, hbb@mek.dtu.dk, rrea@mek.dtu.dk

<sup>2</sup>Department of Mathematical Sciences, Rensselaer Polytechnic Institute, New York

henshw@rpi.edu

## 1 Introduction

The potential-flow finite-difference model of [1] applied a  $\sigma$ -transform in the vertical direction in order to solve for fully nonlinear water wave propagation over varying water depths. This model was also applied to wave-structure interaction problems using the *immersed boundary method*, see for example [2]. In this abstract we present a similar finite-difference model for wave-structure interaction problems which abandons the  $\sigma$ -transform and instead applies *moving and deformable overset grids*. The computational grid in this model is updated according to the nonlinear free-surface motion, and the exact position of the body where the no-flux boundary condition is applied. It is expected that the presented overlapping grid methodology provides more flexibility with respect to grid generation for complicated bodies, especially in three-dimensions (3D). First the accuracy and the convergence of this model is validated using the stream function wave theory. Next the results for the forced motion of a submerged heaving cylinder are compared with the analytical solutions. Note that in this abstract only two-dimensional (2D) results are presented.

## 2 Formulation

A Cartesian coordinate system is adopted, with the origin at the still water level, and the  $z$ -axis pointing vertically upwards. Following the notation of [1], the Laplace equation is written as:

$$\nabla^2\phi + \phi_{zz} = 0, \quad -h < z < \zeta. \quad (2.1)$$

where the horizontal gradient operator is defined by  $\nabla = [\partial/\partial x, \partial/\partial y]$ . The instantaneous free-surface position is  $\zeta$ , and  $h$  is the water depth. The kinematic and dynamic free-surface conditions can also be expressed by:

$$\frac{\partial\zeta}{\partial t} = -\nabla\zeta \cdot \nabla\tilde{\phi} + \tilde{w} (1 + \nabla\zeta \cdot \nabla\zeta), \quad (2.2)$$

$$\frac{\partial\tilde{\phi}}{\partial t} = -g\zeta - \frac{1}{2}\nabla\tilde{\phi} \cdot \nabla\tilde{\phi} + \frac{1}{2}\tilde{w}^2 (1 + \nabla\zeta \cdot \nabla\zeta). \quad (2.3)$$

Here  $\tilde{\phi} = \phi(\mathbf{x}, \zeta, t)$  in which  $\mathbf{x} = [x, y]$  is a horizontal vector, and  $\tilde{w} = \frac{\partial\phi}{\partial z}|_{z=\zeta}$ . A no-flux boundary condition is also defined by  $\mathbf{n} \cdot \nabla\phi = V_n$  at the solid boundaries of the domain with the normal vectors given by  $\mathbf{n}$  and  $V_n$  the normal velocity of the boundary.

## 3 Numerical Method

According to the *Method of Lines*, the spacial and temporal discretization in this model are carried out separately [1]. Using a 4th order finite-difference method, the Laplace equation (2.1) is solved in the computational grid which is comprised of a number of moving and deformable overset grids. An example of the domain is shown in Figure 1. This overset grid has 3 components shown as  $\mathbf{G}_1$ ,  $\mathbf{G}_2$  and  $\mathbf{G}_3$ . The free-surface grid  $\mathbf{G}_3$  is deformable and can be generated using a *Hyperbolic Grid Generation*

technique by marching the *start curve*  $\mathbf{S}_f$  downwards in the  $z$  direction. The component  $\mathbf{G}_2$  represents the grid for a circular submerged cylinder. This grid can be moved depending on the desired body boundary condition on  $\mathbf{S}_B$  at each time step. The background grid  $\mathbf{G}_1$  is fixed and only changes in the overlapping regions. The start curve  $\mathbf{S}_f$  (free-surface) is marched in time using the classical explicit 4th-order Runge-Kutta integration scheme. This is performed by calculation of the solution slopes for elevation  $\zeta$  and velocity potential  $\tilde{\phi}$  from (2.2) and (2.3). The whole overset grid and the overlapping region is updated accordingly at each time step. The velocity potential at the free surface  $\mathbf{S}_f$  specifies a Dirichlet condition for the Laplace problem. The body boundary condition is also applied as a non-homogeneous Neumann condition on  $\mathbf{S}_B$ . All spacial discretizations are performed using centered stencils and 2 layers of ghost points are added for each component grid. This computational strategy is implemented inside **Overture** [3].

## 4 Results and discussions

### 4.1 Stream function theory

The stream function wave theory of [4] is used in this section to verify the convergence of the presented model. The computational grid for this case is made of only  $\mathbf{G}_3$  and  $\mathbf{G}_1$  in Figure 1. The initial conditions for  $\zeta$  and  $\tilde{\phi}$  at  $\mathbf{S}_f$  are specified from the solution to the stream function theory. At both left and right boundaries of the grid, periodic conditions are applied. The computed solution for the surface elevation  $\zeta$  after 5 wave periods is compared with the analytical results. See Figure 2 and Figure 3. The results are shown for increasing wave steepness in the range  $H/\lambda = 0.02, 0.04, \dots, 0.10, 0.11, 0.126$ . In all these cases  $kh = 2\pi$ . Here  $H$  is the wave height,  $\lambda$  is the wave length and  $k = 2\pi/\lambda$  is the wave number. Note also that a mild filter at each time step is applied on  $\tilde{\phi}$  and  $\zeta$  to ensure numerical stability for the steep wave cases. As can be seen from the figure, the dispersion error increases with the wave steepness.

### 4.2 Forced oscillation of submerged cylinder

For this case, a submerged circular cylinder with radius  $a$  is forced to oscillate in the vertical direction. The submergence depth is  $\hat{h} = 3a$ . The computational grid is shown in Figure 1. Note that for this grid at the far end of the domain for both  $\mathbf{G}_3$  and  $\mathbf{G}_1$  a homogeneous Neumann condition is considered. The oscillation amplitude is in the range  $\eta/a = 0.2, 0.4, \dots, 1.00, 1.25, 1.50, 1.75$ . The grid in Figure 1 is part of the solution for the extreme case with  $\eta/a = 1.75$ . The frequency of the forced motion  $\omega$  is also specified as  $\nu a = 1.0$ , where  $\nu = \omega^2/g$ . The applied force on the body is calculated in time as:

$$F_z = -\rho \int_{\mathbf{S}_B} \left( \frac{\partial \phi}{\partial t} + \frac{1}{2} \nabla \phi \cdot \nabla \phi \right) n_z dS, \quad (4.1)$$

where  $\rho$  is the density of water. A harmonic analysis is then performed to find the amplitudes of the force harmonics. The results are compared with the analytical solution in [5], and are shown in

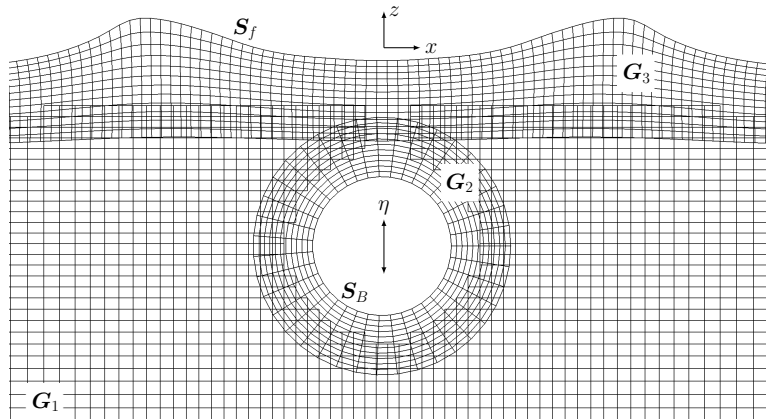


Figure 1: The deformable and moving overset grid. The grid is for the case where a submerged circular cylinder is performing forced oscillation  $\eta$  in the  $z$  direction.

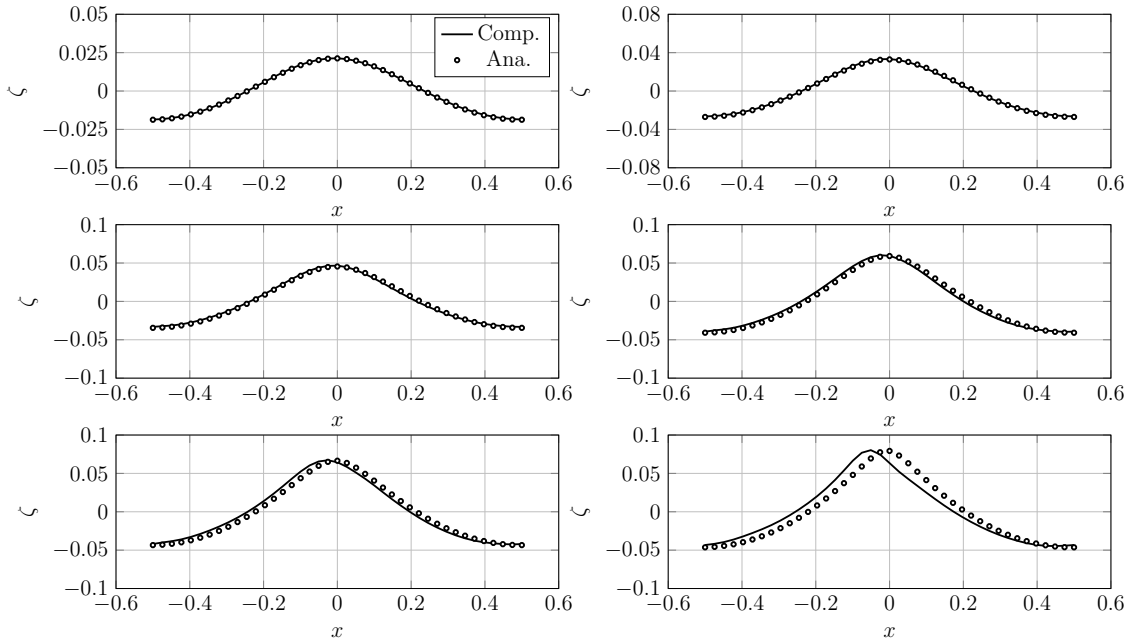


Figure 2: Comparison between the computed free-surface wave elevation  $\zeta$  with the analytical results from the stream function theory. The results are for increasing steepness, and are obtained after 5 wave periods. The extreme case shown in the bottom right plot is for the wave at 80 % of the breaking limit. For all these cases  $kh = 2\pi$ .

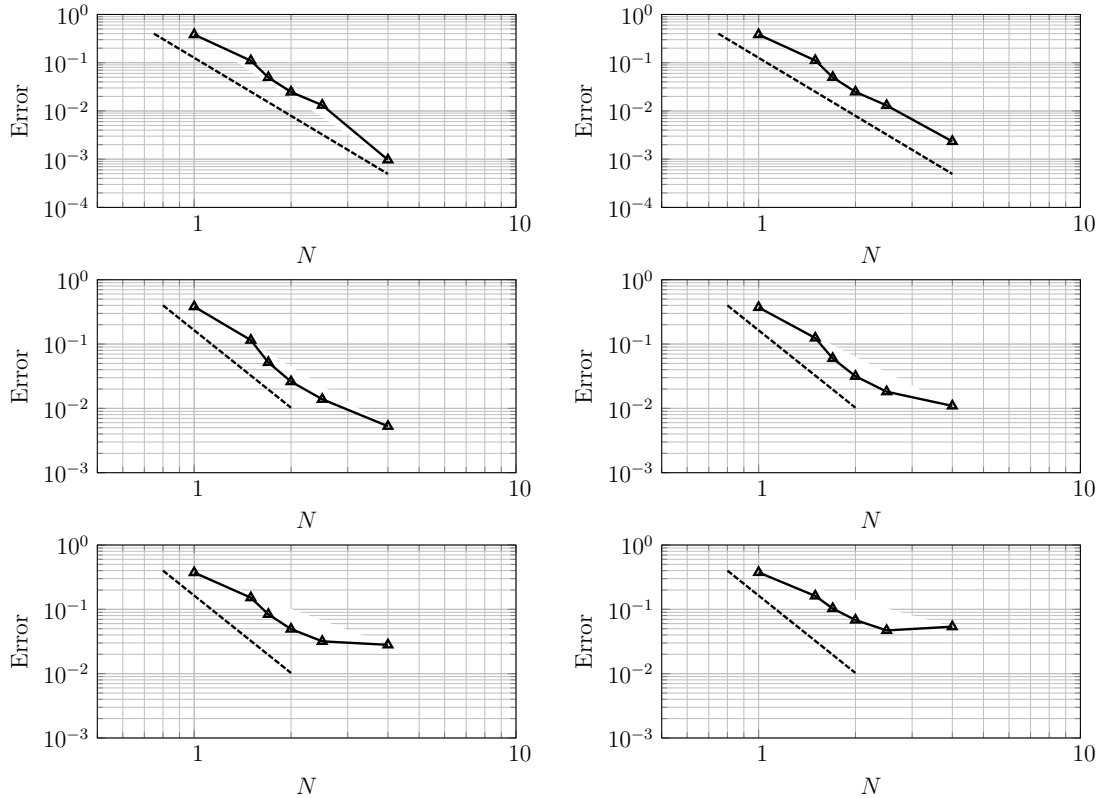


Figure 3: Convergence studies for the cases shown in Figure 2. The dashed lines in the plots show 1 to 4 slope. Note that  $N = 1$  represents the computational grid with  $Nx = 11$  and  $Nz = 14$  number of grid points. The resolution study is performed by  $N = [1 \ 1.5 \ 1.7 \ 2 \ 2.5 \ 4]$ . The plots in Figure 2 are for the case with  $N = 4$ .

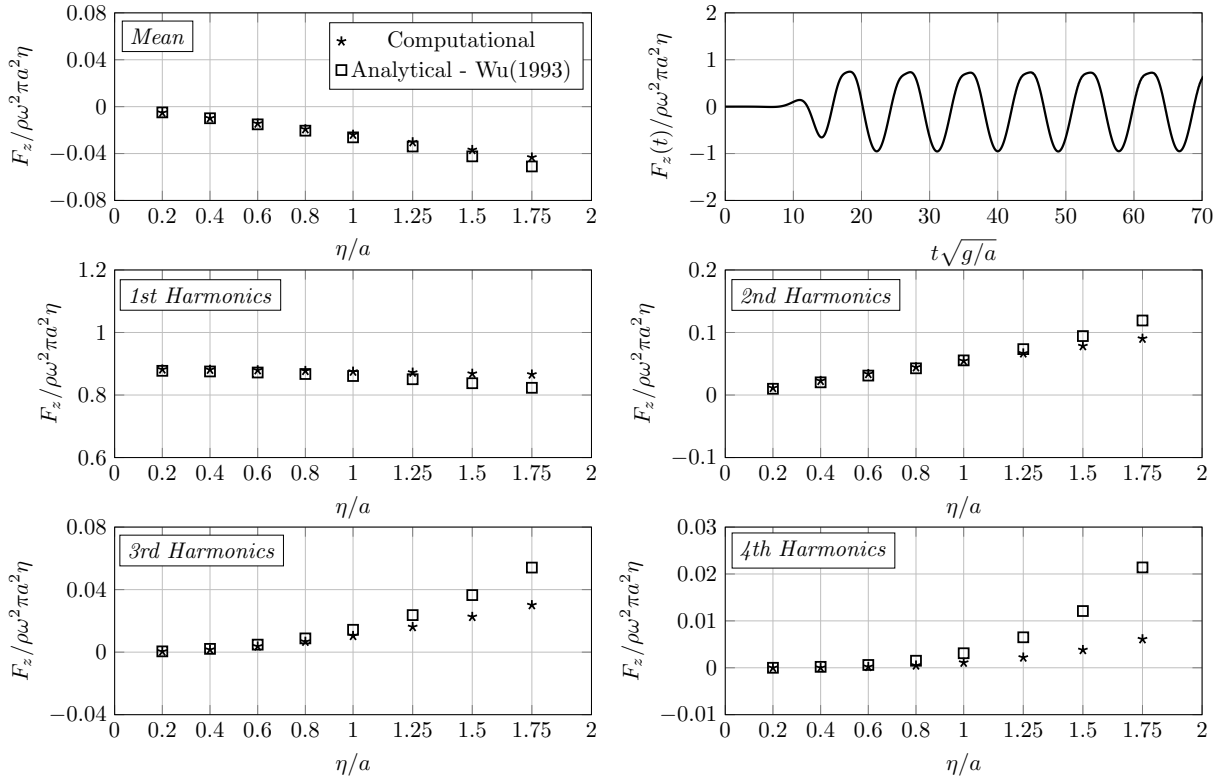


Figure 4: Amplitudes of the force harmonics due to the forced motion of the submerged cylinder. The top right plot shows an example of applied force in time which is for the extreme case  $\eta/a = 1.75$ .

Figure 4. Note also that the analytical solution in [5] is based on the linear free surface conditions. This fact may explain the discrepancies between the solutions for the large motion amplitudes, and we are currently running this case in order to verify or refute this supposition.

## 5 Conclusions

A new computational strategy has been presented based on moving and deformable overset grids for the wave-structure interaction problem solved by finite-differences. The accuracy and the convergence of the model has been investigated by comparison to stream function wave theory. The results for the force harmonics due to forced motion of the submerged cylinder are also compared with analytical results, and good agreement has been shown for small amplitude motions.

## Acknowledgement

The Danish Maritime Fund and The Orients Fund are greatly appreciated for their financial support.

## References

- [1] H. B. Bingham and H. Zhang, "On the accuracy of finite-difference solutions for nonlinear water waves," *Journal of Engineering Mathematics*, vol. 58, no. 1-4, pp. 211–228, 2007.
- [2] S. Kontos, H. B. Bingham, O. Lindberg, and A. P. Engsig-Karup, "On nonlinear wave-structure interaction using an immersed boundary method in 2D," in *31th International Workshop on Water Waves and Floating Bodies (IWWF 2016)*, 2016.
- [3] D. L. Brown, W. D. Henshaw, and D. J. Quinlan, "Overture: An object-oriented framework for solving partial differential equations on overlapping grids," *Object Oriented Methods for Interoperable Scientific and Engineering Computing, SIAM*, pp. 245–255, 1999.
- [4] J. Fenton, "The numerical solution of steady water wave problems.," *Comp. Geosci.*, vol. 14, no. 3, pp. 357–368, 1988.
- [5] G. Wu, "Hydrodynamic forces on a submerged circular cylinder undergoing large-amplitude motion," *Journal of Fluid Mechanics*, vol. 254, pp. 41–58, 1993.